Electronic Supplementary Information

for

Double B←N Bridged Bipyridine-Containing Polymer Acceptors with Enhanced Electron Mobility for All-Polymer Solar Cells

Xiaojing Long,*[,a] Jiuyong Yao,[a] Fangfang Cheng,[a] Chuandong Dou,*[,b] and Yanzhi Xia[a]

[a] *State Key Laboratory of Bio-Fibers and Eco-Textiles, Shandong Collaborative Innovation Center of Marine Biobased Fibers and Ecological textiles, College of Materials Science and Engineering, Institute of Marine Biobased Materials, Qingdao University, Qingdao 266071, China.*

[b] *State Key Laboratory of Polymer Physics and Chemistry, Changchun Institute of Applied Chemistry, Chinese Academy of Sciences, Changchun, 130022, P. R. China*

* Corresponding authors:

longxj@qdu.edu.cn (X. Long); chuandong.dou@ciac.ac.cn (C. Dou)

Contents

1. Thermal properties

The thermal properties of **P-BNBP-2f** and **P-BNBP-4f** were determined by thermogravimetric analysis (TGA) in N_2 flow. They show good thermal stability with thermal decomposition temperature (T_d) at 5% weight loss of 350 ^oC.

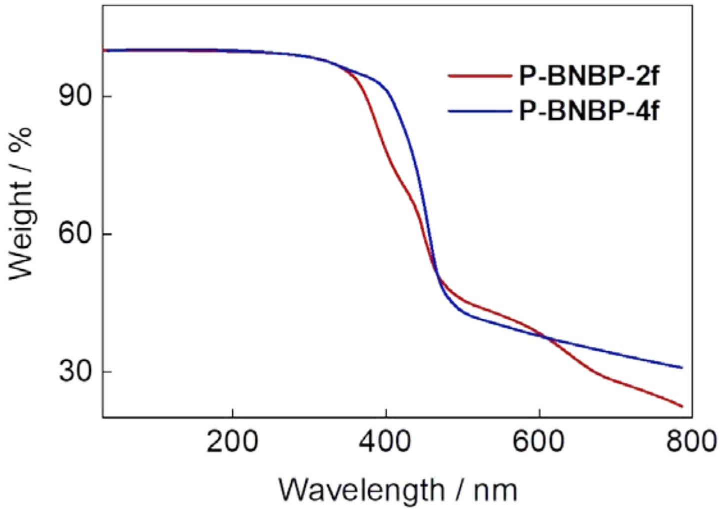

Figure S1. TGA curves of **P-BNBP-2f** and **P-BNBP-4f**.

2. Theoretical calculations

The structural optimizations and DFT calculations of the model compounds **P-BNBP-2f** and **P-BNBP-4f** were performed using Gaussian 09 program at the B3LYP/6-31G(d,p) level of theory[1]. **P-BNBP-2f** and **P-BNBP-4f** contain four repeating units with the long alkyl chains on BNBP are replaced by the methyl groups.

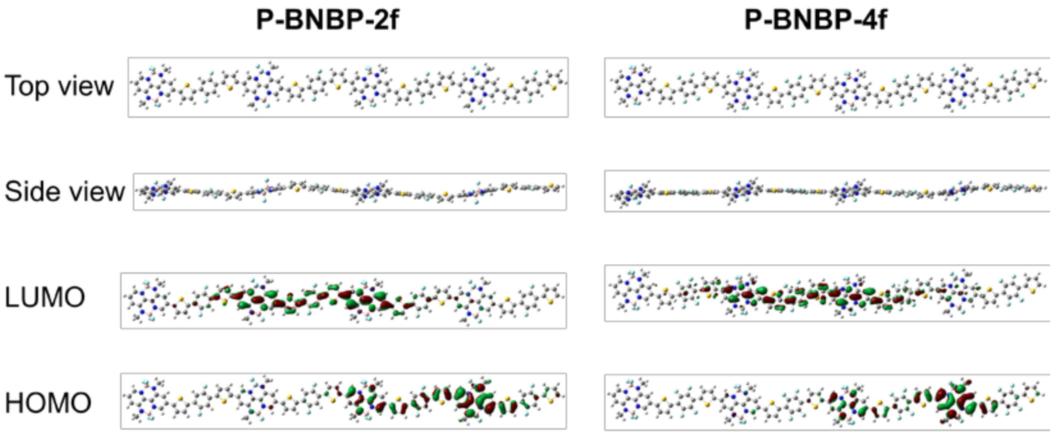

Figure S2. The optimized structures and Kohn-Sham LUMOs and HOMOs of the model compounds of **P-BNBP-2f** and **P-BNBP-4f**.

3. Electron mobilities

The electron/hole mobilities were measured using the space-charge-limited current (SCLC) method based on the *J*-*V* curves of the electron-only/hole-only devices. The electron-only device structure is ITO/PEIE/Active layer/Ca/Al and the hole-only device structure is ITO/PEDOT:PSS/Active layer/MoO_3/Al. The *J*-*V* curves in the range of 0–10 V were recorded using a computer-controlled Keithley 2400 source meter, and the results were fitted to a space-charge limited function:

$$J = \frac{9}{8}\varepsilon_r\varepsilon_0\mu\frac{V^2}{L^3}\exp\left(0.89\beta\frac{\sqrt{V}}{\sqrt{L}}\right)$$

where J is the current density, ε_0 is the permittivity of free space, ε_r is the relative permittivity of 3 for conjugated polymers, μ is the zero-field mobility, V is the potential across the device ($V = V_{applied}–V_{bias}–V_{series}$), L is the thickness of active layer, and β is the field-activation factor. The series and contact resistance (V_{series}) of the device (10–15 Ω) were measured using blank device of ITO/PEIE/Ca/Al or ITO/PEDOT:PSS/MoO_3/Al.

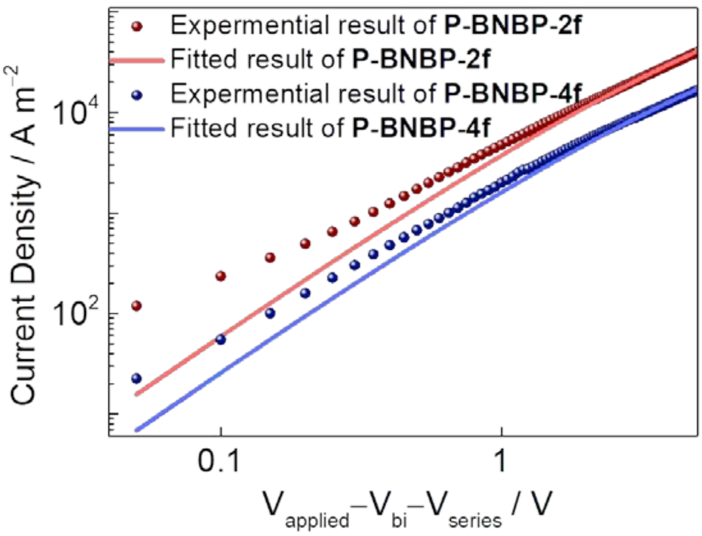

Figure S3. Space-charge-limited current (SCLC) fittings of the electron-only devices based on the thin films of **P-BNBP-2f** and **P-BNBP-4f**.

4. Photophysical and electrochemical properties

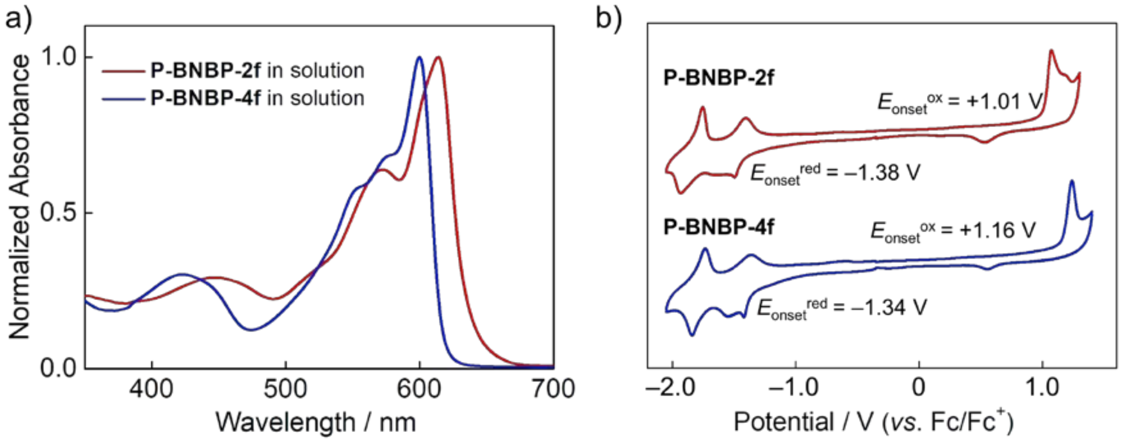

Figure S4. a) UV−Vis absorption spectra of **P-BNBP-2f** and **P-BNBP-4f** in solutions at 25 ºC. b) Cyclic voltammograms of **P-BNBP-2f** and **P-BNBP-4f**; Fc = ferrocene.

5. All-PSC device performance and characterizations

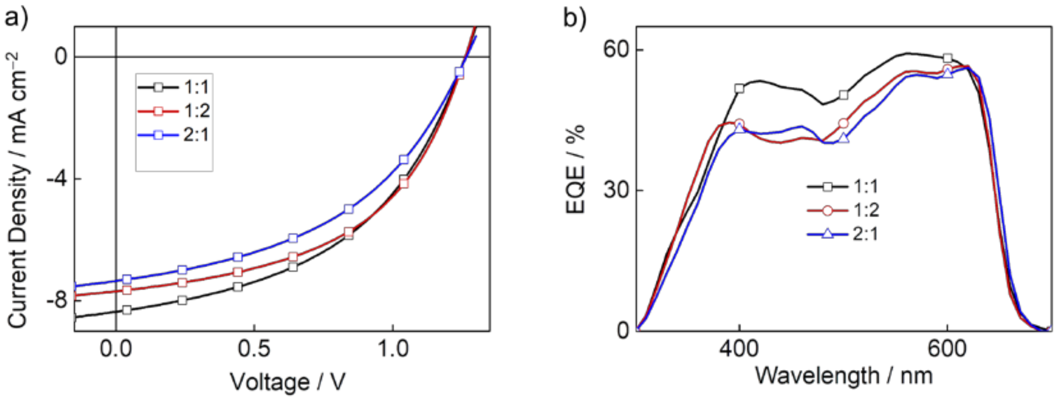

Figure S5. a) *J–V* curves and b) EQE spectra of the all-PSC devices based on the J61:**P-BNBP-2f** blend in CF solution with various ratios.

Table S1. Device performance of the all-PSC devices based on the J61:**P-BNBP-2f** blend in CF solution with various ratios.

Donor:Acceptor	V_{oc} (V)	J_{sc} (mA cm^{-2})	FF	PCE (%)
1:1	1.26	8.37	0.47	4.92
1:2	1.26	7.70	0.50	4.84
2:1	1.27	7.35	0.45	4.19

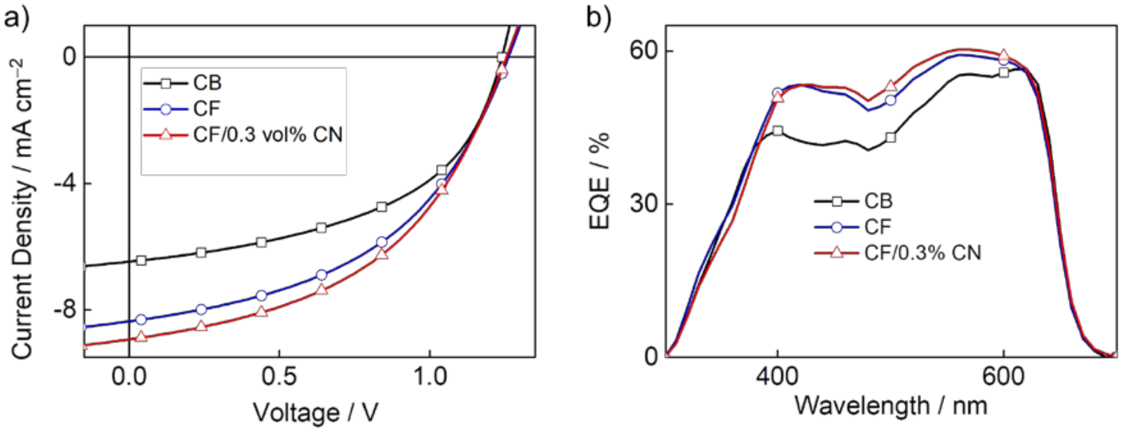

Figure S6. a) *J–V* curves and b) EQE spectra of the all-PSCs based-on the J61:**P-BNBP-2f** blends in CB, CF and CF with 0.3 vol% CN, respectively.

Table S2. Device performance of the all-PSCs based-on the J61:**P-BNBP-2f** blends in CB, CF and CF with 0.3 vol% CN, respectively.

Solvents	V_{oc} (V)	J_{sc} (mA cm^{-2})	FF (%)	PCE (%)
CB	1.24	6.48	0.50	4.03
CF	1.26	8.37	0.47	4.92
CF/0.3 vol% CN	1.26	8.93	0.47	5.26

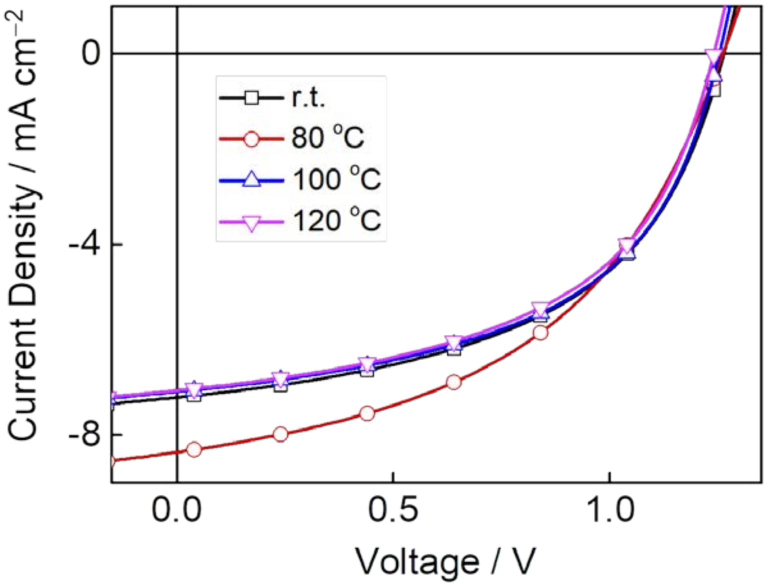

Figure S7. *J–V* curves of the all-PSCs based-on the J61:**P-BNBP-2f** blend in CF solution with different annealing temperatures.

Table S3. Device performance of the all-PSCs based-on the J61:**P-BNBP-2f** blend in CF solution with different annealing temperatures.

Annealing temperature (°C)	V_{oc} (V)	J_{sc} (mA cm^{-2})	FF (%)	PCE (%)
r.t.	1.26	7.21	0.52	4.68
80	1.26	8.37	0.47	4.92
100	1.25	7.09	0.52	4.64
120	1.24	7.07	0.52	4.53

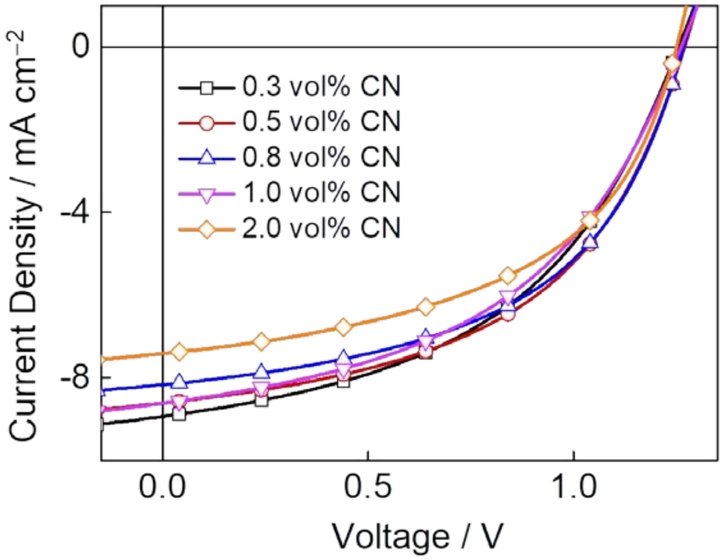

Figure S8. *J–V* curves of the all-PSCs based-on the J61:**P-BNBP-2f** blend in CF solution with CN additive.

Table S4. Device performance of the all-PSCs based-on the J61:**P-BNBP-2f** blend in CF solution with CN additive.

Additive content (vol %)	V_{OC} (V)	J_{SC} (mA cm^{-2})	FF (%)	PCE (%)
0	1.26	8.37	0.47	4.92
0.3	1.26	8.93	0.47	5.26
0.5	1.27	8.61	0.50	5.46
0.8	1.27	8.18	0.51	5.32
1.0	1.26	8.61	0.47	5.06
2.0	1.25	7.41	0.51	4.70

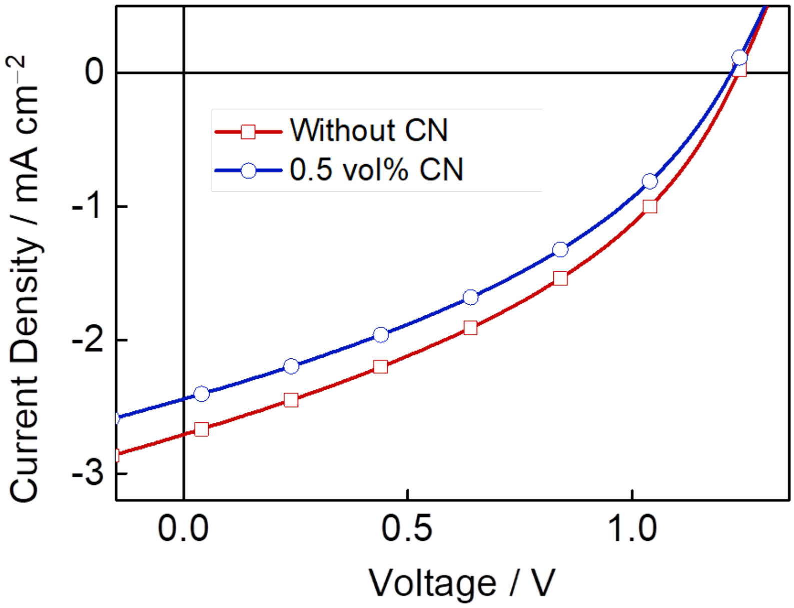

Figure S9. *J*–*V* curves of the all-PSCs based-on the J61:**P-BNBP-4f** blend in CF solution with or without CN additive.

Table S5. Device performance of the all-PSCs based-on the J61:**P-BNBP-4f** blend in CF solution with or without CN additive.

Additive content vol %	V_{oc} (V)	J_{sc} (mA cm^{-2})	FF (%)	PCE (%)
0	1.24	2.70	0.39	1.30
0.5	1.22	2.44	0.38	1.12

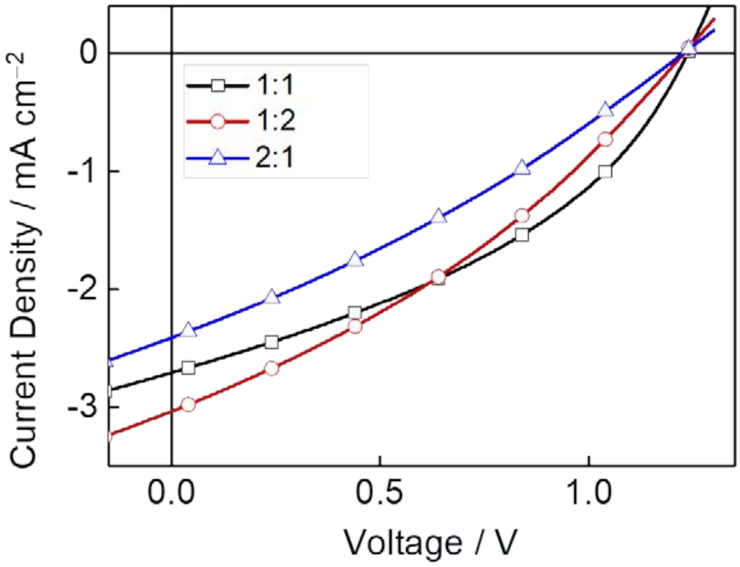

Figure S10. *J*–*V* curves of the all-PSCs based-on the J61:**P-BNBP-4f** blend in CF solution with various ratios.

Table S6. Device performance of the all-PSCs based-on the J61:**P-BNBP-4f** blend in CF solution with various ratios.

Donor:Acceptor	V_{oc} (V)	J_{sc} (mA cm^{-2})	FF (%)	PCE (%)
1:1	1.24	2.70	0.39	1.30
1:2	1.23	3.04	0.33	1.22
2:1	1.23	2.41	0.30	0.89

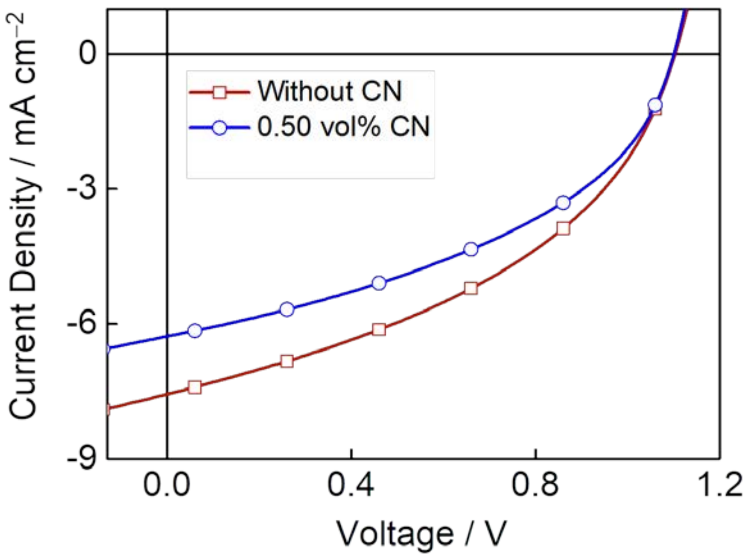

Figure S11. *J–V* curves of the all-PSCs based-on the PBDTTT-E-T:**P-BNBP-2f** blend in CF solution with or without CN additive.

Table S7. Device performance of the all-PSCs based-on the PBDTTT-E-T:**P-BNBP-2f** blend in CF solution with or without CN additive.

Additive content (vol %)	V_{OC} (V)	J_{SC} (mA cm^{-2})	FF	PCE (%)
0	1.10	7.56	0.42	3.51
0.5	1.10	6.27	0.43	2.94

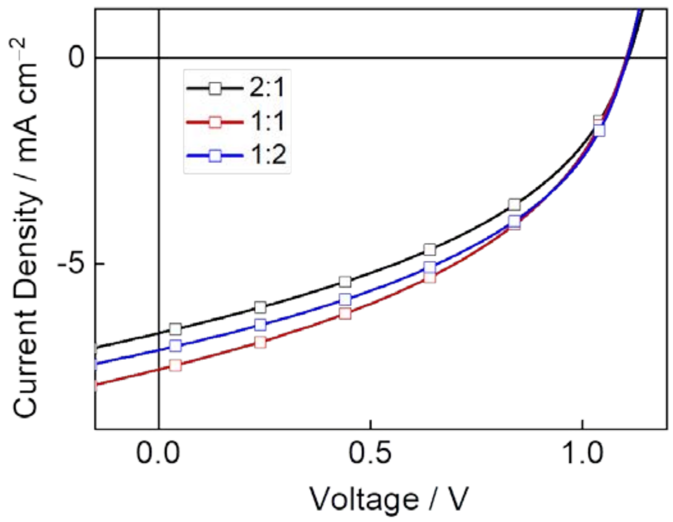

Figure S12. *J*–*V* curves of the all-PSCs based-on the J61:**P-BNBP-4f** blend in CF solution with various ratios.

Table S8. Device performance of the all-PSCs based-on the J61:**P-BNBP-4f** blend in CF solution with various ratios.

Donor:Acceptor	V_{OC} (V)	J_{SC} (mA cm^{-2})	FF	PCE (%)
1:1	1.10	7.56	0.42	3.51
1:2	1.11	7.09	0.43	3.39
2:1	1.11	6.68	0.41	3.08

Table S9. Device statistics of the optimized all-PSCs device performance.[a]

Donor:acceptor	V_{OC} (V)	J_{SC} (mA cm^{-2})	FF	PCE (%)
J61:**P-BNBP-2f**	1.27±0.005	8.61±0.14	0.50±0.02	5.46±0.20
PBDTTT-E-T:**P-BNBP-2f**	1.10±0.01	7.56±0.10	0.42±0.01	3.51±0.04
J61:**P-BNBP-4f**	1.24±0.003	2.71±0.15	0.39±0.01	1.30±0.15
PBDTTT-E-T:**P-BNBP-4f**	1.11±0.002	1.18±0.18	0.28±0.01	0.36±0.18

[a]Average±standard deviation.

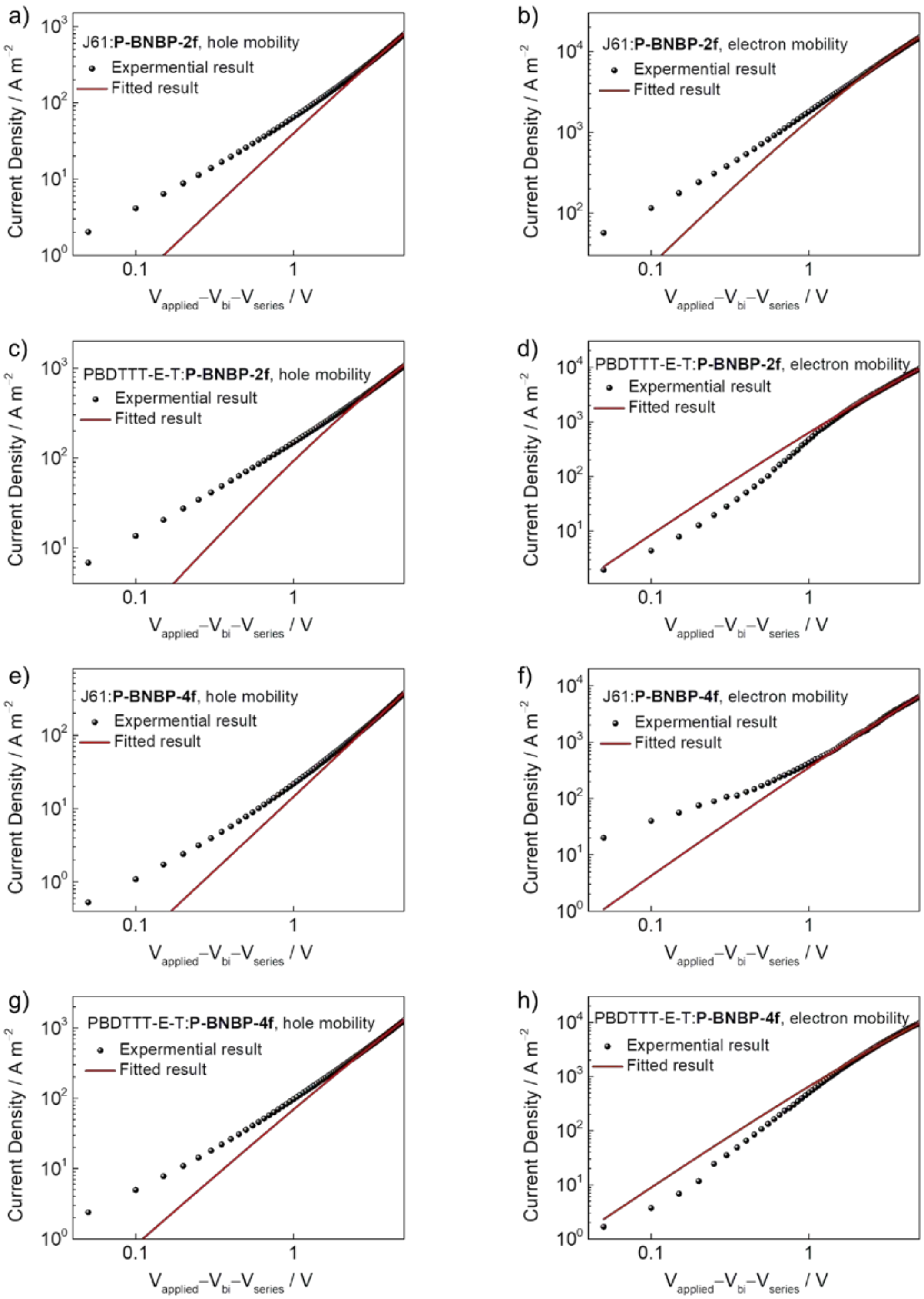

Figure S13. SCLC fittings of the hole-only devices of a) J61:**P-BNBP-2f**, c) PBDTTT-E-T:**P-BNBP-2f**, e) J61:**P-BNBP-4f** as well as g) PBDTTT-E-T:**P-BNBP-4f** blend films and electron-only devices of b) J61:**P-BNBP-2f**, d) PBDTTT-E-T:**P-BNBP-2f**, f) J61:**P-BNBP-4f** as well as h) PBDTTT-E-T:**P-BNBP-4f** blend films.

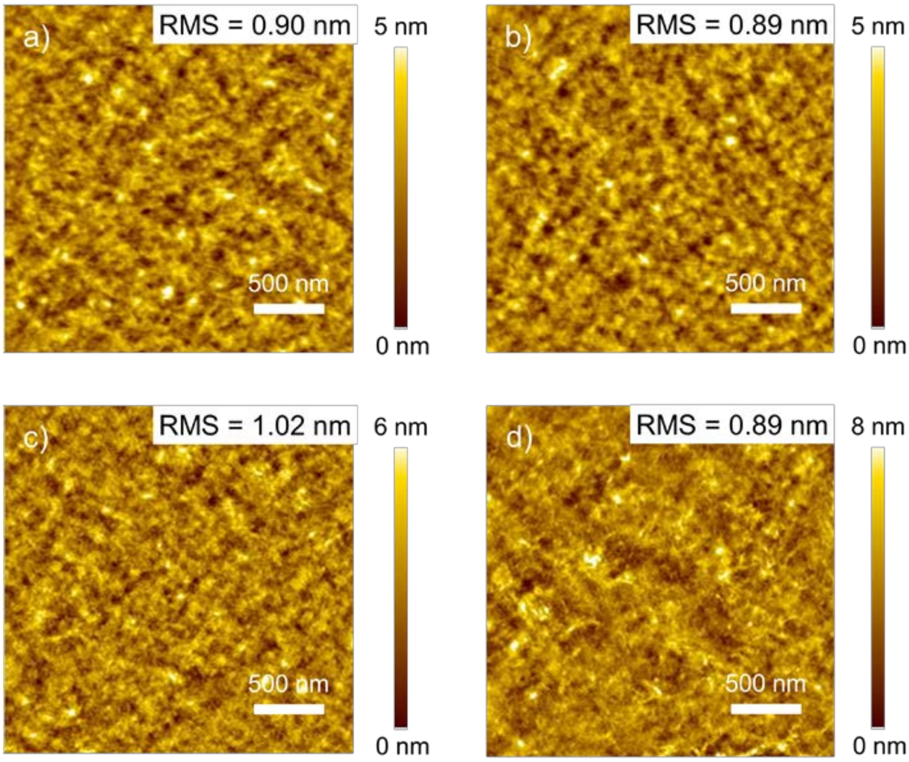

Figure S14. The AFM images of the active layers: a) the J61:**P-BNBP-2f** blend; b) the PBDTTT-E-T:**P-BNBP-2f** blend; c) the J61:**P-BNBP-4f** blend and d) the PBDTTT-E-T:**P-BNBP-4f** blend.

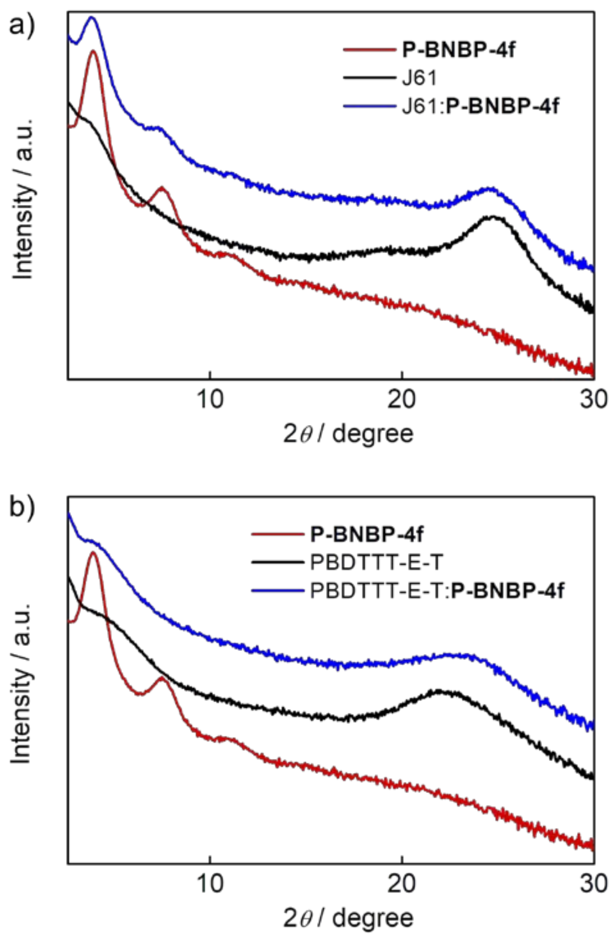

Figure S15. The GI-XRD patterns of the polymer pristine films and the polymer blend films based on a) **P-BNBP-4f** and J61; b) **P-BNBP-4f** and PBDTTT-E-T.

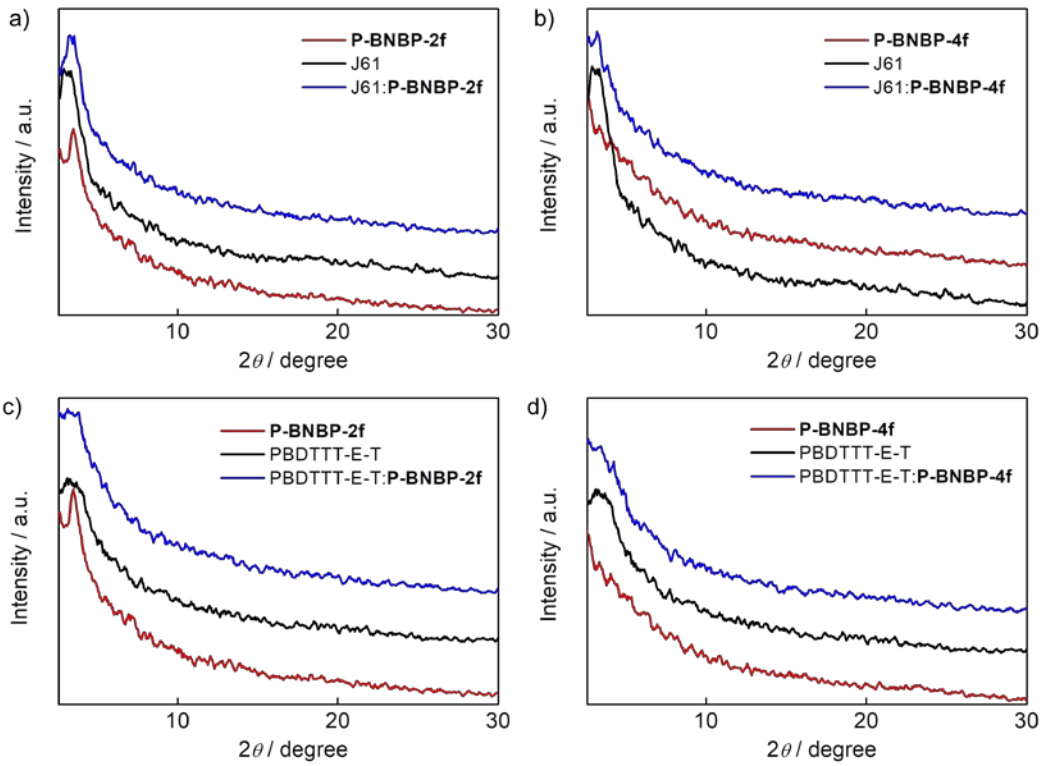

Figure S16. The IP-XRD patterns of the polymer pristine films and the polymer blend films based on a) **P-BNBP-2f** and J61; b) **P-BNBP-4f** and J61; c) **P-BNBP-2f** and PBDTTT-E-T; d) **P-BNBP-4f** and PBDTTT-E-T.

6. ¹H NMR spectra

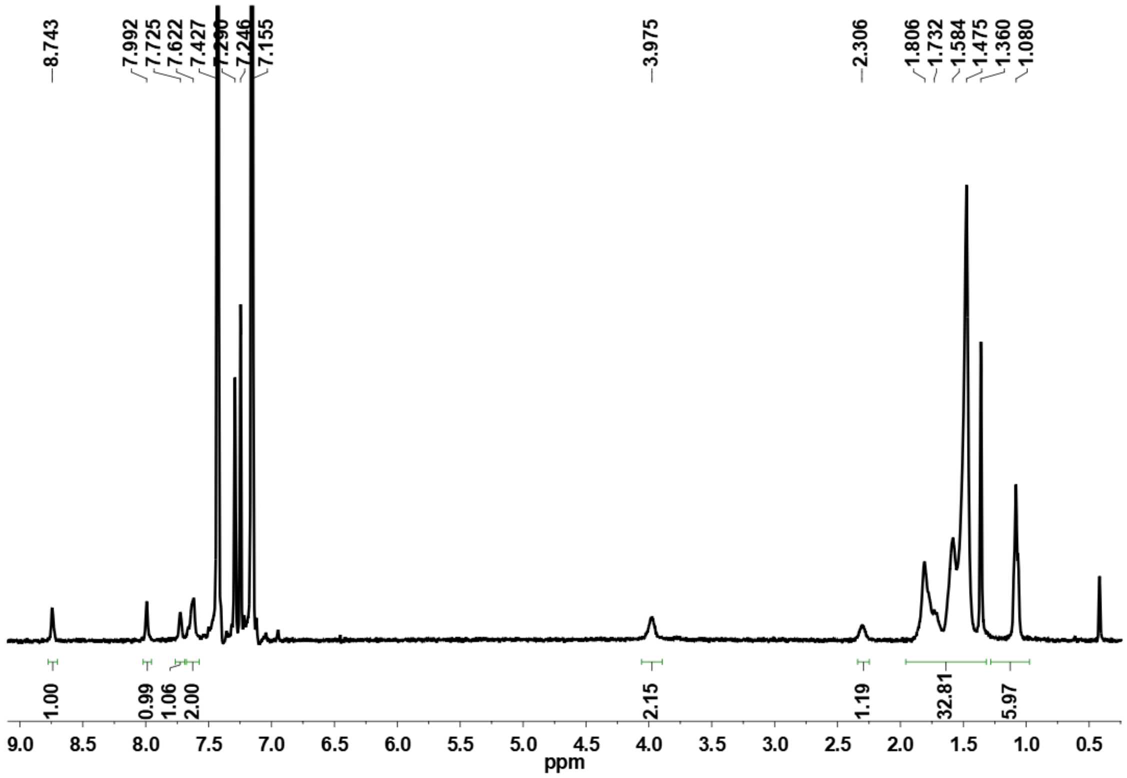

Figure S17. ¹H NMR spectrum of **P-BNBP-2f**.

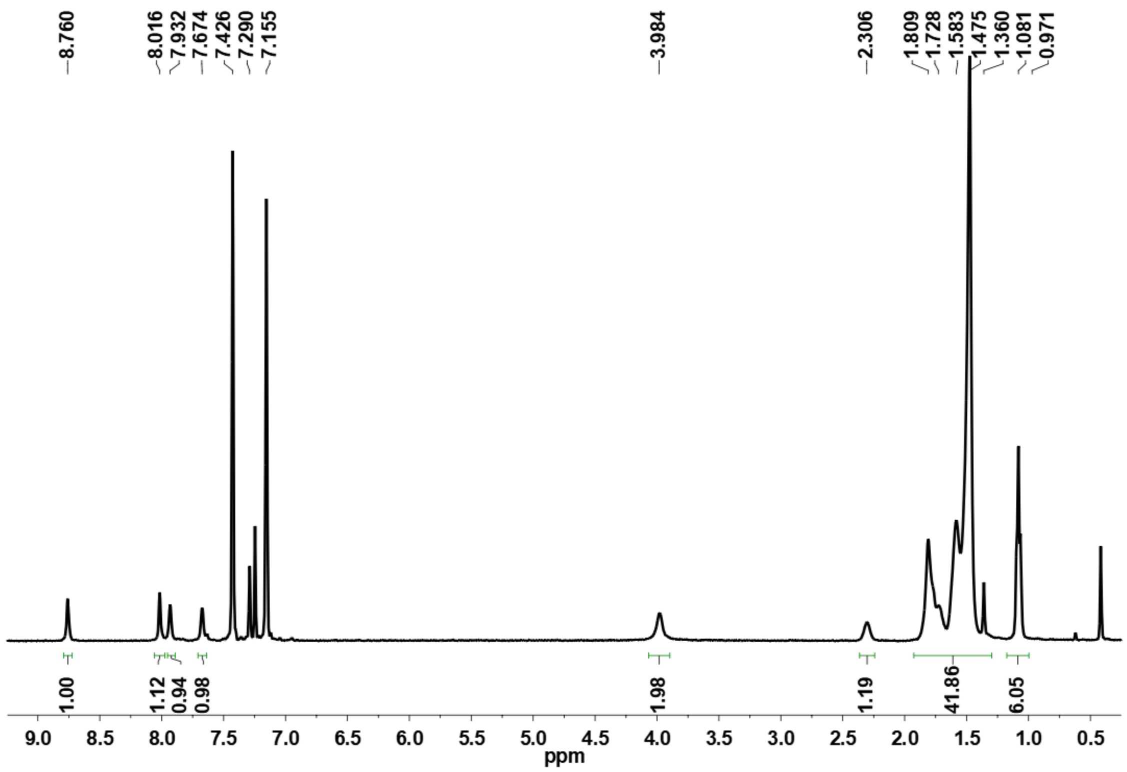

Figure S18. ¹H NMR spectrum of **P-BNBP-4f**.

7. Reference

[1] Gaussian 09 (Revision A.02), M. J. Frisch, G. W. Trucks, H. B. Schlegel, G. E. Scuseria, M. A. Robb, J. R. Cheeseman, G. Scalmani, V. Barone, B. Mennucci, G. A. Petersson, H. Nakatsuji, M. Caricato, X. Li, H. P. Hratchian, A. F. Izmaylov, J. Bloino, G. Zheng, J. L. Sonnenberg, M. Hada, M. Ehara, K. Toyota, R. Fukuda, J. Hasegawa, M. Ishida, T. Nakajima, Y. Honda, O. Kitao, H. Nakai, T. Vreven, J. A. Montgomery, Jr., J. E. Peralta, F. Ogliaro, M. Bearpark, J. J. Heyd, E. Brothers, K. N. Kudin, V. N. Staroverov, R. Kobayashi, J. Normand, K. Raghavachari, A. Rendell, J. C. Burant, S. S. Iyengar, J. Tomasi, M. Cossi, N. Rega, J. M. Millam, M. Klene, J. E. Knox, J. B. Cross, V. Bakken, C. Adamo, J. Jaramillo, R. Gomperts, R. E. Stratmann, O. Yazyev, A. J. Austin, R. Cammi, C. Pomelli, J. W. Ochterski, R. L. Martin, K. Morokuma, V. G. Zakrzewski, G. A. Voth, P. Salvador, J. J. Dannenberg, S. Dapprich, A. D. Daniels, Ö. Farkas, J. B. Foresman, J. V. Ortiz, J. Cioslowski, D. J. Fox, Gaussian, Inc., Wallingford CT, 2009.